Research Article Vol. 5, No. 9 / September 2018 / Optica 1091

Superpositions of up to six plane waves without electric-field interference

K. C. van Kruining,[1,*] R. P. Cameron,[2] and J. B. Götte[3,4]

[1]Max Planck Institute for the Physics of Complex Systems, Nöthnitzer Straße 38, 01187 Dresden, Germany
[2]University of Strathclyde, 107 Rottenrow East, G4 0NG Glasgow, UK
[3]Nanjing University, 22 Hankou Road, Nanjing 210093, China
[4]University of Glasgow, University Avenue, G12 8QQ Glasgow, UK
*Corresponding author: koen@pks.mpg.de

Received 4 June 2018; revised 30 July 2018; accepted 10 August 2018 (Doc. ID 334161); published 10 September 2018

Superpositions of coherent light waves typically interfere. We present superpositions of up to six plane waves that defy this expectation by having a perfectly homogeneous mean square of the electric field. For many applications in optics, these superpositions can be seen as having a homogeneous intensity. Our superpositions show interesting one-, two-, and three-dimensional patterns in their helicity densities, including several that support bright regions of superchirality. Our superpositions might be used to write chiral patterns in certain materials, and, conversely, such materials might be used as the basis of an "optical helicity camera" capable of recording spatial variations in helicity.

https://doi.org/10.1364/OPTICA.5.001091

1. INTRODUCTION

The electric and magnetic fields of a plane electromagnetic wave are orthogonal to each other and the direction of propagation. This suggests that the maximum number of waves with the same frequency that can be superposed without any interference is three. This can be done by choosing three waves travelling in mutually orthogonal directions and choosing all three polarizations orthogonal to each other.

If one is content with only the mean square of the electric field being homogeneous without requiring that the mean square of the magnetic field also be homogeneous, larger superpositions are allowed. For many practical purposes, such superpositions can still be considered noninterfering, as it is the electric field that interacts most with matter, including fluorescent dyes, CCDs, and the light-sensitive pigments in the human eye. The inhomogeneity in the magnetic field is relatively difficult to detect.

The helicity density, a quantity that indicates the handedness of the light [1–5], is in general inhomogeneous for our noninterfering superpositions. It will vary in space in a pattern that is quite often, although not necessarily, periodic and resembles the intensity variations in optical lattices. There is enough freedom left in our superpositions to allow for a large variety of helicity lattices.

Some noninterfering superpositions show superchirality, an effect introduced by Tang and Cohen [6–8]. Superchiral light has regions where the helicity density is much higher than one would expect from the local mean square of the electric field. The key difference is that other superchiral superpositions exploit interference to create a region where the mean square of the electric field is weak, but the mean square of the magnetic field is not, allowing for the helicity density to become very large compared to the squared local electric field [6,9]. The helicity is actually quite small compared to the squared electric field outside of this "dark region." Alternatively, plasmonic resonators have been proposed to generate high helicities close to a surface [10–14]. Noninterfering superpositions achieve superchirality in free space and in "bright regions" where the mean square of the electric field is not suppressed.

This paper is structured as follows. In Section 2 we show how to construct noninterfering superpositions. We then give several examples along with their helicity density patterns in Section 3. In Section 4 we estimate the residual inhomogeneity of the mean square of the electric field under small deviations from the exact required parameters. In Section 5 we discuss the possibility of recording the helicity density patterns of our noninterfering superpositions using chirally sensitive liquid crystals, and in Section 6 we discuss several open mathematical questions related to noninterfering superpositions.

2. CONSTRUCTION OF NONINTERFERING SUPERPOSITIONS AND THEIR HELICITY PROPERTIES

In this paper we work in the classical domain in free space and consider non-trivial superpositions of N plane electromagnetic waves, each of which has the same angular frequency $\omega = ck$. For a superposition of N waves, the resulting electric and magnetic fields are

$$\mathbf{E} = \mathrm{Re}\,\tilde{\mathbf{E}} = \mathrm{Re}\left(\sum_{j=1}^{N} \tilde{\mathbf{E}}_j e^{i(\mathbf{k}_j\cdot\mathbf{x}-\omega t)}\right), \tag{1}$$

$$\mathbf{H} = \mathrm{Re}\,\tilde{\mathbf{H}} = \mathrm{Re}\left(\frac{1}{\mu_0\omega}\sum_{j=1}^{N} \mathbf{k}_j \times \tilde{\mathbf{E}}_j e^{i(\mathbf{k}_j\cdot\mathbf{x}-\omega t)}\right).$$

By a non-trivial superposition, we mean $\mathbf{k}_i \neq \mathbf{k}_j \quad \forall\, i \neq j$ and $\tilde{\mathbf{E}}_j \neq 0 \quad \forall\, j$. The complex amplitudes $\tilde{\mathbf{E}}_j$ define the polarizations, amplitudes, and phases of the waves. Because light's polarization is transverse, $\tilde{\mathbf{E}}_j \cdot \mathbf{k}_j = 0 \quad \forall\, j$ applies.

A. Interference Cancellation

The mean square of the electric field is given by

$$\frac{\omega}{2\pi}\int_0^{\frac{2\pi}{\omega}} \mathbf{E}\cdot\mathbf{E}dt = \frac{1}{2}\tilde{\mathbf{E}}\cdot\tilde{\mathbf{E}}^* = \frac{1}{2}\left(\sum_{l=1}^{N}\tilde{\mathbf{E}}_l\cdot\tilde{\mathbf{E}}_l^* + \sum_{j=1}^{N}\sum_{l\neq j}\tilde{\mathbf{E}}_j\cdot\tilde{\mathbf{E}}_l^* e^{i(\mathbf{k}_j-\mathbf{k}_l)\cdot\mathbf{x}}\right). \tag{2}$$

If this is to be homogeneous, the second sum must vanish. The most obvious way to achieve this is to choose the constituent plane waves such that no two interfere, in which case $\tilde{\mathbf{E}}_j \cdot \tilde{\mathbf{E}}_l^* = 0 \quad \forall\, j \neq l$. This can be done for at most three plane waves because there are three orthogonal polarization directions possible. In this paper we recognize that it is also possible, however, to allow multiple pairs of waves to interfere, provided the associated interference patterns cancel. To appreciate this, suppose that there exists within the superposition a pair $(j \neq l)$ of interfering waves, with the spatial periodicity of the associated interference pattern being dictated by the wavevector difference $\mathbf{k}_j - \mathbf{k}_l$. If another pair $(j' \neq l')$ of interfering waves with the same wavevector difference $\mathbf{k}_j - \mathbf{k}_l = \mathbf{k}_{j'} - \mathbf{k}_{l'}$ can be identified, giving an associated interference pattern with the same spatial periodicity, then the two interference patterns will cancel provided that $\tilde{\mathbf{E}}_j \cdot \tilde{\mathbf{E}}_l^* + \tilde{\mathbf{E}}_{j'} \cdot \tilde{\mathbf{E}}_{l'}^* = 0$. The same reasoning applies for more than two pairs of interfering waves with the same wavevector difference. It is this trick that allows us to superpose more than three plane waves while keeping the mean square of the electric field homogeneous.

B. Optical Helicity and Helicity Lattices

The definition of helicity density stems from plasma physics [15] and is known for arbitrary light fields in vacuum [1–4,16] and for an arbitrary medium with linear response [17]. As we are considering only monochromatic light fields, we can use the simpler expression $\mathcal{H} = \frac{1}{2}\,\mathrm{Im}(\tilde{\mathbf{E}}\cdot\tilde{\mathbf{H}}^*)/c\omega$. The helicity density is bounded between $\pm\frac{1}{4\omega}(\epsilon_0\tilde{\mathbf{E}}\cdot\tilde{\mathbf{E}}^* + \mu_0\tilde{\mathbf{H}}\cdot\tilde{\mathbf{H}}^*)$. For a superposition of N plane waves, one has

$$\mathcal{H} = \frac{-i}{4c\omega}\sum_{i,j=1}^{N}(\tilde{\mathbf{E}}_i\cdot\tilde{\mathbf{H}}_j^* - \tilde{\mathbf{E}}_j^*\cdot\tilde{\mathbf{H}}_i)e^{i(\mathbf{k}_i-\mathbf{k}_j)\cdot\mathbf{x}}. \tag{3}$$

When all waves are linearly polarized, the terms with $i = j$ are zero and only the "interference terms" remain. The vectors $\mathbf{k}_i - \mathbf{k}_j$ of all nonzero terms determine if the helicity density forms a lattice. If they are all linear combinations with integer coefficients of $\dim(\mathrm{span}\{\mathbf{k}_i - \mathbf{k}_j | \tilde{\mathbf{E}}_i\cdot\tilde{\mathbf{H}}_j^* - \tilde{\mathbf{E}}_j^*\cdot\tilde{\mathbf{H}}_i \neq 0\})$ vectors, they form a lattice. If not, they form a less regular structure. Here, span{} Is the space spanned by a set of vectors, and dim() is the dimension.

The superchirality threshold is $\sqrt{\epsilon_0\mu_0}|\mathrm{Im}(\tilde{\mathbf{E}}\cdot\tilde{\mathbf{H}}^*)| > \epsilon_0\tilde{\mathbf{E}}^*\cdot\tilde{\mathbf{E}}$ [6]. Because $\tilde{\mathbf{E}}^*\cdot\tilde{\mathbf{E}}$ is homogeneous by design for all examples we will give, the occurrence of superchirality implies a stronger inequality, which we take as a sufficient condition for "bright superchirality": $\max(\sqrt{\epsilon_0\mu_0}|\mathrm{Im}(\tilde{\mathbf{E}}\cdot\tilde{\mathbf{H}}^*)|) > \max(\epsilon_0\tilde{\mathbf{E}}^*\cdot\tilde{\mathbf{E}})$ (max = maximum). That is, the local helicity is large compared to the squared electric field anywhere. To the best of our knowledge, no monochromatic electromagnetic field with this property has ever been identified.

3. EXPLICIT EXAMPLES

In this section our graphics of the helicity structure will always be 4×4 or $4\times4\times4$ wavelengths large unless stated otherwise, and we use blue for negative helicity and red for positive helicity.

We will show diagrams to illustrate the superpositions for which we plot the helicity density. In these diagrams, gray arrows indicate wavevectors and electric field polarizations are indicated with yellow arrows. Green arrows to indicate the magnetic polarizations are included for reference, as well. Mutually cancelling pairs of interference terms are indicated by red lines, and interference terms contributing to the inhomogeneous helicity density are shown as black dashed lines.

In every example we will give of a noninterfering superposition, there is some freedom left to change the amplitudes and propagation directions of the different waves. We will use a_j to indicate free complex amplitudes, which can take any nonzero value, and θ_j and ϕ_j to indicate free angles, where $0 \leq \theta_j < \pi$ and $0 \leq \phi_j < 2\pi$, unless additional constraints are mentioned. An overall rotation of all wave and polarization vectors keeps a noninterfering superposition trivially noninterfering and we will not include this freedom in our parametrizations. Sometimes it is useful for convenient viewing of the helicity plots to include an overall rotation. We will indicate when we do this.

We observe the strongest superchirality when all free amplitudes have roughly the same magnitude, although one can typically vary them by a factor of 2 or more before superchirality completely disappears. This is only a rule of thumb, because optimizing a superposition for maximal superchirality is complicated and beyond the scope of this paper.

A. Two Waves

Two plane waves can always be orthogonally polarized regardless of what their wavevectors are. One way to achieve this is to choose the polarization of one wave to lie in the plane spanned by the wavevectors of both waves and the other one orthogonal to this plane [5,18]. It is convenient to choose both waves to lie in the x–y plane, symmetrically with respect to the y axis (see Table 1).

For this configuration, $\tilde{\mathbf{E}}\cdot\tilde{\mathbf{E}}^*$ and $\tilde{\mathbf{H}}\cdot\tilde{\mathbf{H}}^*$ are homogeneous. If one computes the helicity density, however, one does find a fringe

Table 1. Two-Wave Noninterfering Superposition

j	$\mathbf{k}_j$	$\tilde{\mathbf{E}}_j$
1	$[\sin\theta, \cos\theta, 0]$	$a_1[0, 0, 1]$
2	$[-\sin\theta, \cos\theta, 0]$	$a_2[\cos\theta, \sin\theta, 0]$

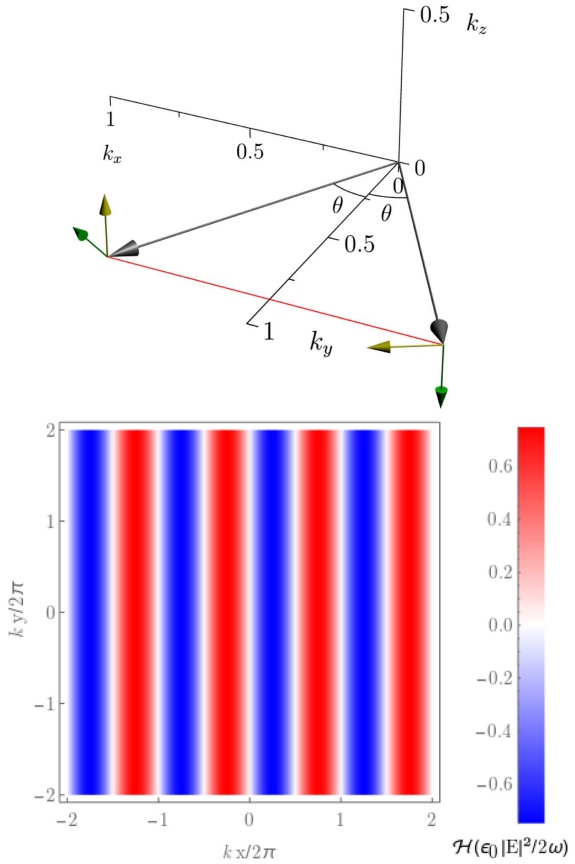

Fig. 1. Wave- and polarization vectors for a noninterfering two-wave superposition (top) and its helicity pattern (bottom). For this superposition we chose both amplitudes equal and $\theta = \pi/6$.

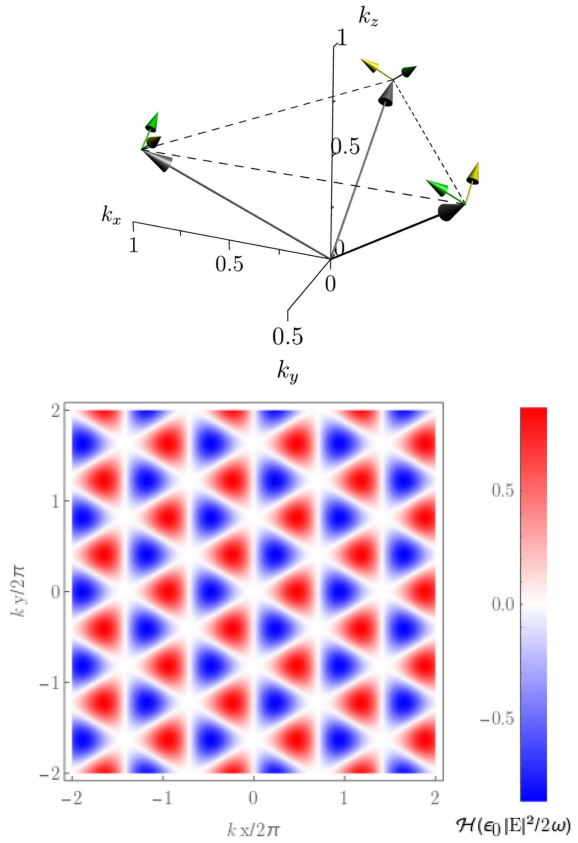

Fig. 2. Wave and polarization vectors for three noninterfering orthogonal waves ($\phi_1 = \phi_2 = \phi_3 = 0$), with all amplitudes taken equal (top) and their helicity structure (bottom). For three plane waves, the helicity interference terms always lie in a plane and thus form a two-dimensional helicity lattice. The wavevectors have been rotated to make the helicity lattice lie on the x–y plane.

structure similar to intensity interference fringes one would get if one chose the polarizations parallel (see Fig. 1):

$$\mathcal{H} = -\frac{\epsilon_0}{\omega}|a_1 a_2^*|\cos^2\theta\,\sin(k_0\,\sin(2\theta)x + \arg(a_1 a_2^*)). \quad (4)$$

Because of the helicity-dependent force it exerts on chiral molecules [18,19] and birefringent microparticles [20,21], this superposition has been studied in some detail. It has been found to act like a matter wave grating on chiral molecules [22], similar to how a standing light wave can act like a grating for molecules in general [23–25].

B. Three Waves

Having three waves travelling in orthogonal directions and with orthogonal polarizations yields both homogeneous $\tilde{\mathbf{E}}\cdot\tilde{\mathbf{E}}^*$ and $\tilde{\mathbf{H}}\cdot\tilde{\mathbf{H}}^*$. This setup already shows an interesting helicity structure, forming a triangular lattice, as is shown in Fig. 2. One is free to change the relative amplitudes. This will alter the shape of the positive and negative helicity regions within a unit cell, but keeps the lattice vectors fixed.

If only $\tilde{\mathbf{E}}^*\cdot\tilde{\mathbf{E}}$ has to be constant, but $\tilde{\mathbf{H}}^*\cdot\tilde{\mathbf{H}}$ may vary, one can construct more superpositions by rotating the wavevectors of the three waves around axes given by their polarization directions; see Table 2.

The additional freedom one gets from only requiring $\tilde{\mathbf{E}}^*\cdot\tilde{\mathbf{E}}$ to be homogeneous allows for a larger variety of helicity structures, including ones that are superchiral, as shown in Fig. 3.

Table 2. Three-Wave Noninterfering Superposition

j	$\mathbf{k}_j$	$\tilde{\mathbf{E}}_j$
1	$[\cos\phi_1, 0, -\sin\phi_1]$	$a_1[0, 1, 0]$
2	$[-\sin\phi_2, \cos\phi_2, 0]$	$a_2[0, 0, 1]$
3	$[0, -\sin\phi_3, \cos\phi_3]$	$a_3[1, 0, 0]$

C. Four Waves

For superposing four waves without electric-field interference, one has to cancel a pair of interference terms against each other. One can take all wavevectors lying in a plane with their tips on the corners of a rectangle. If one takes one pair of waves polarized out of the plane and the other two polarized in plane, there is only one nonzero pair of interference terms. One can then adjust the phases and amplitudes to make this pair of interference terms cancel. Taking all wavevectors in the x–y plane, we parameterize the waves as shown in Table 3.

The helicity density of this superposition is zero for $\theta < \frac{\pi}{4}$ because both helicity terms cancel. For $\frac{\pi}{4} < \theta < \frac{\pi}{2}$, the helicity structure consists of sinusoidal fringes along the x axis, a pattern that can already be achieved by superposing two waves [20,22].

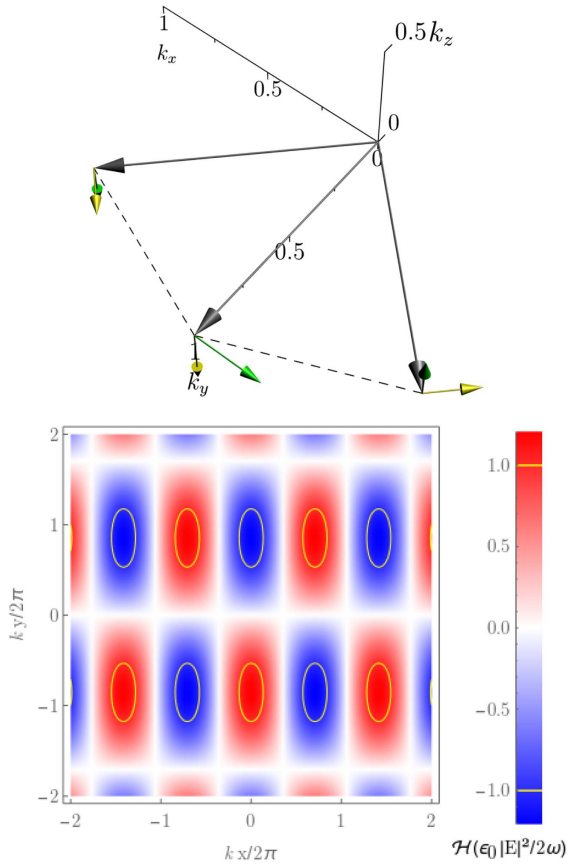

Fig. 3. Construction of a superchiral three-wave superposition (top). We have taken $\phi_1 = 0$, $\phi_2 = \frac{7\pi}{4}$, and $\phi_3 = \frac{3\pi}{2}$, rotated to make the helicity lattice vectors parallel to the x and y axes. We took a_2 to be $\sqrt{2}$ times the amplitude of the other waves. The corresponding helicity structure (bottom) has superchiral regions (yellow ellipses), which extend for about half a wavelength in one direction and a quarter of a wavelength in the other.

Table 3. Four-Wave Noninterfering Superposition with All Wavevectors in the Same Plane[a]

j	$\mathbf{k}_j$	$\tilde{\mathbf{E}}_j$
1	$[\cos\theta,\ \sin\theta, 0]$	$a_1[0, 0, 1]$
2	$[\cos\theta,\ -\sin\theta, 0]$	$a_2[0, 0, 1]$
3	$[-\cos\theta,\ \sin\theta, 0]$	$-\frac{a_1 a_2^* \,\mathrm{sgn}(\cos 2\theta)}{a_4^* \sqrt{\lvert\cos 2\theta\rvert}}[\sin\theta,\ \cos\theta, 0]$
4	$[-\cos\theta,\ -\sin\theta, 0]$	$\frac{a_4}{\sqrt{\lvert\cos 2\theta\rvert}}[-\sin\theta,\ \cos\theta, 0]$

[a]The angle θ can be anything between 0 and $\frac{\pi}{2}$ except $\frac{\pi}{4}$.

One can also take two waves lying in the x–y plane and polarized in the z direction and two waves travelling in the y–z plane polarized in the x direction. If both pairs of waves travel at the same relative angle, one can choose the amplitudes and phases such that their interference terms cancel; see Table 4.

The helicity pattern of this superposition consists again of sinusoidal fringes, but this superposition allows for a fifth wave to be added while keeping the mean square of the electric field constant. This five-wave superposition will be treated in the next subsection.

Table 4. Four-Wave Noninterfering Superposition with Two Pairs of Wave Vectors in Perpendicular Planes [a]

j	$\mathbf{k}_j$	$\tilde{\mathbf{E}}_j$
1	$[\cos\theta,\ \sin\theta, 0]$	$a_1[0, 0, 1]$
2	$[\cos\theta,\ -\sin\theta, 0]$	$a_2[0, 0, 1]$
3	$[0,\ \sin\theta,\ \cos\theta]$	$-\frac{a_1 a_2^*}{a_4^*}[1, 0, 0]$
4	$[0,\ -\sin\theta,\ \cos\theta]$	$a_4[1, 0, 0]$

[a]A fifth wave can be added to this superposition while keeping the mean square electric field homogeneous; see Table 6.

There exists another four-wave superposition that involves the cancellation of two pairs of interference terms. It is constructed by taking a pair of waves travelling in orthogonal directions (we take them symmetric with respect to the z axis) polarized in the plane spanned by the wavevectors. Then add a second copy of this pair rotated around the bisector of the first pair with an additional relative phase of π between them; see Table 5.

The helicity lattice formed by this superposition shows rhombs of positive and negative helicity arranged in a rectangular lattice, as is shown in Fig. 4. Superchirality occurs when a_1 and a_3 are of comparable magnitude.

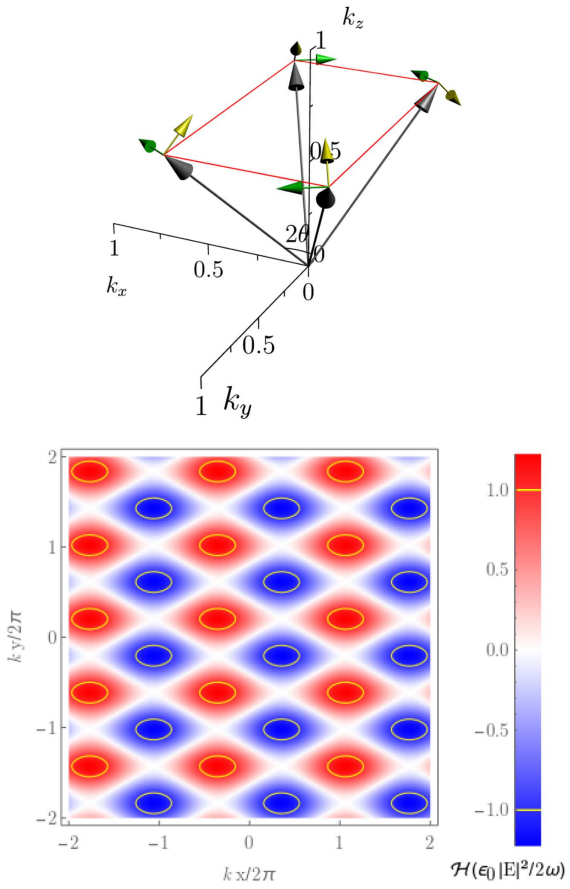

Fig. 4. Four-wave noninterfering superposition with two pairs of cancelling interference terms (top) and its helicity structure (bottom). For this superposition we chose $a_1 = a_3$, $\theta = \frac{\pi}{6}$, and $\Delta\phi = 0$. Superchirality is typical for superpositions of this kind and occurs over broad parameter ranges.

Table 5. Four-Wave Noninterfering Superposition Which Has Superchiral Helicity Lattices

j	$\mathbf{k}_j$	$\tilde{\mathbf{E}}_j$
1	$\frac{\sqrt{2}}{2}[\cos\theta, \sin\theta, 1]$	$a_1\frac{\sqrt{2}}{2}[-\cos\theta, -\sin\theta, 1]$
2	$\frac{\sqrt{2}}{2}[-\cos\theta, -\sin\theta, 1]$	$a_1^*\frac{a_3}{a_3^*}e^{i\Delta\phi}\frac{\sqrt{2}}{2}[-\cos\theta, -\sin\theta, -1]$
3	$\frac{\sqrt{2}}{2}[-\cos\theta, \sin\theta, 1]$	$a_3\frac{\sqrt{2}}{2}[\sin\theta, -\cos\theta, 1]$
4	$\frac{\sqrt{2}}{2}[\cos\theta, -\sin\theta, 1]$	$a_3e^{i\Delta\phi}\frac{\sqrt{2}}{2}[-\sin\theta, \cos\theta, 1]$

Table 6. Five-Wave Noninterfering Superposition

j	$\mathbf{k}_j$	$\tilde{\mathbf{E}}_j$
1	$[\cos\theta, \sin\theta, 0]$	$a_1[0, 0, 1]$
2	$[\cos\theta, -\sin\theta, 0]$	$a_2[0, 0, 1]$
3	$[0, \sin\theta, \cos\theta]$	$-\frac{a_1a_2^*}{a_4^*}[1, 0, 0]$
4	$[0, -\sin\theta, \cos\theta]$	$a_4[1, 0, 0]$
5	$[\cos\phi, 0, \sin\phi]$	$a_5[0, 1, 0]$

D. Five Waves

The five-wave superposition we found is the only one we know about with a genuine three-dimensional helicity structure. It is constructed the following way. Take two plane waves propagating in the x–y plane polarized in the z direction. Take two plane waves in the y–z plane propagating at the same relative angles and polarized in the x direction. By choosing the amplitudes and phases of these waves right, one can cancel the interference terms between these waves, as explained in the previous subsection. Then one can add a fifth wave propagating in the x–z plane polarized in the y direction. The parameters of this superposition are shown in Table 6.

As one can see in Fig. 5, the wavevectors lie on the corners of a (generically skewed) pyramid. The difference vectors between them form the sides of the pyramid. One can write all these difference vectors as linear combinations with integer coefficients of only three of them, choosing two that lie in the base and one connecting the base to the apex. Therefore, the helicity structure of this superposition is generically periodic. For generic parameters, the helicity lattice is monoclinic, with higher lattice symmetries for special parameters. If one chooses $\phi = \frac{\pi}{4} \vee \frac{5\pi}{4}$, the apex of the pyramid lies directly above the center of the base, and the helicity lattice is orthorhombic. If the base of the pyramid is a square, as well, the helicity lattice is tetragonal. This is the case for $\theta = \arccos\frac{2}{\sqrt{6}}$.

For the special cases $\phi = \frac{3\pi}{2} + \operatorname{arctg}(1 - \cos\theta)$ or $\phi = \pi - \operatorname{arctg}(1 - \cos\theta)$ all difference vectors between the wavevectors lie in the same plane and the helicity structure is generically aperiodic, except if they all are rational linear combinations of only two of them, which happens for $\cos\theta/\sqrt{2}\,\sin(\operatorname{arctg}(1 - \cos\theta)) \in \mathbb{Q}$. If this condition is met, the helicity structure is a two-dimensional rectangular lattice, although the unit cell may be very large depending on the precise ratio.

The large number of free parameters this superposition has allows one to construct superchiral helicity lattices with surprisingly pronounced (≈1.4 times the threshold value) and large (extending about half a wavelength in two directions) superchiral regions. We found that the most pronounced superchirality is achieved when the fifth wave points in roughly the same direction as the total momentum of the other four, whereas having it point in the opposite direction attenuates the helicity modulations to far below the superchirality threshold.

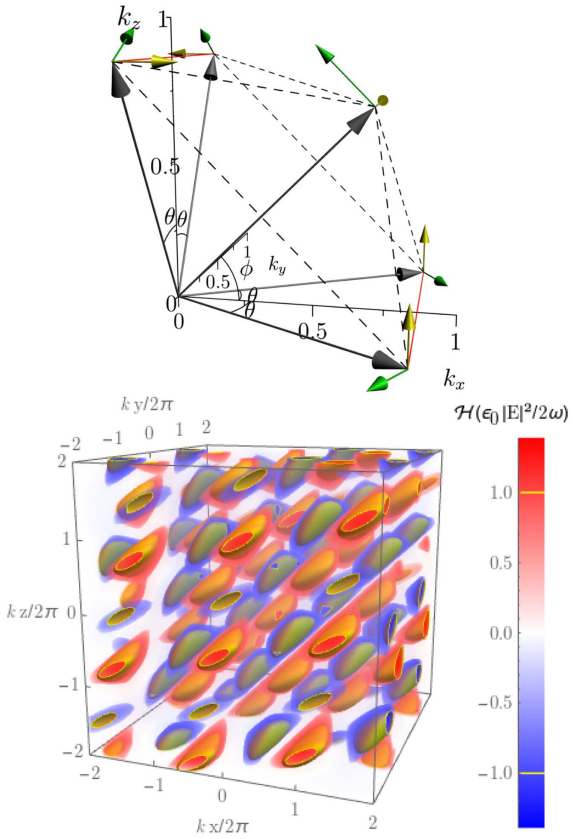

Fig. 5. Example of a five-wave noninterfering superposition (top) yielding a three-dimensional helicity lattice (bottom). For this superposition we took $\theta = \frac{\pi}{6}$, $\phi = \frac{\pi}{4}$, $a_1 = a_2 = a_4 = 1$, and $a_5 = \sqrt[4]{8}\sqrt{\cos\pi/6}$. The superchiral regions are enclosed by the yellow surfaces. At about half a wavelength in length they are surprisingly large.

E. Six Waves

One can superpose six waves by having three cancelling pairs of interference terms. The superposition is constructed by putting the six wavevectors on the corners of a hexagon. Three of them are polarized in the plane of the hexagon and three perpendicular to it. The plane waves in Table 7 lead to a cancellation of all interference terms.

Because all wavevectors lie in the same plane, the helicity structure is always two dimensional, and with three sets of interference terms contributing to the helicity structure (dashed lines in Fig. 6), it is not in general periodic in all directions, as one can see in Fig. 7. For the helicity structure to be periodic there have to exist two lattice vectors that have all $\mathbf{k}_i - \mathbf{k}_j$, contributing to the helicity structure as linear combinations with integer coefficients. This condition is equivalent to all $\mathbf{k}_i - \mathbf{k}_j$ being linear combinations with rational coefficients of two $\mathbf{k}_i - \mathbf{k}_j$ and is satisfied if $|\cos\theta|/(1 - |\cos\theta|) \in \mathbb{Q}$. There exist an infinite

Table 7. Six-Wave Noninterfering Superposition[a]

j	$\mathbf{k}_j$	$\tilde{\mathbf{E}}_j$
1	$[1, 0, 0]$	$a_1[0, 0, 1]$
2	$[\cos\theta,\ \sin\theta, 0]$	$a_2[0, 0, 1]$
3	$[\cos\theta,\ -\sin\theta, 0]$	$a_3[0, 0, 1]$
4	$[-1, 0, 0]$	$-\frac{a_1^*\sqrt{\lvert\cos 2\theta\rvert}}{\cos\theta}[0,\ -1, 0]$
5	$[-\cos\theta,\ -\sin\theta, 0]$	$\frac{a_2^*}{\sqrt{\lvert\cos 2\theta\rvert}}[\sin\theta,\ -\cos\theta, 0]$
6	$[-\cos\theta,\ \sin\theta, 0]$	$\frac{a_3^*}{\sqrt{\lvert\cos 2\theta\rvert}}[-\sin\theta,\ -\cos\theta, 0]$

[a]Here, θ is limited to the intervals $\frac{\pi}{4} < \theta < \frac{\pi}{2}$ or $\frac{\pi}{2} < \theta < \frac{3\pi}{4}$. By varying the parameters, a large variety of two-dimensional helicity lattices are possible.

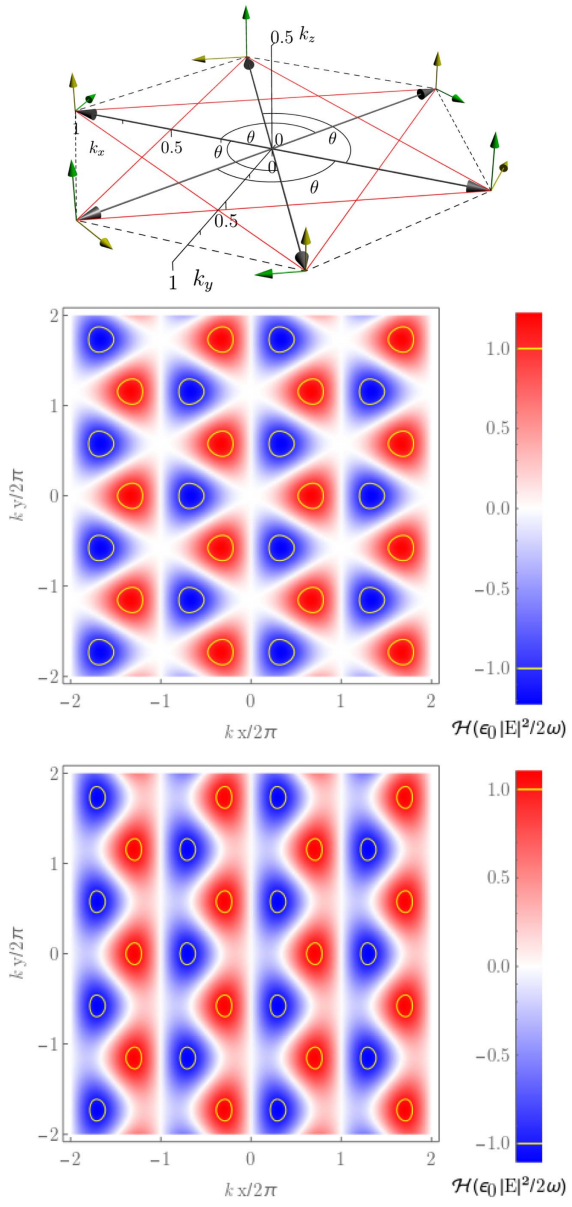

Fig. 6. Six-wave superposition with $\theta = \frac{2\pi}{3}$ (top). This superposition requires three pairs of interference terms to cancel. For $\theta = \frac{2\pi}{3}$, the helicity forms a triangular lattice. Two examples are shown, one for $a_1 = a_2 = a_3$ (center) and one for $a_1 = \frac{1}{2}a_2 = \frac{1}{2}a_3$ (bottom).

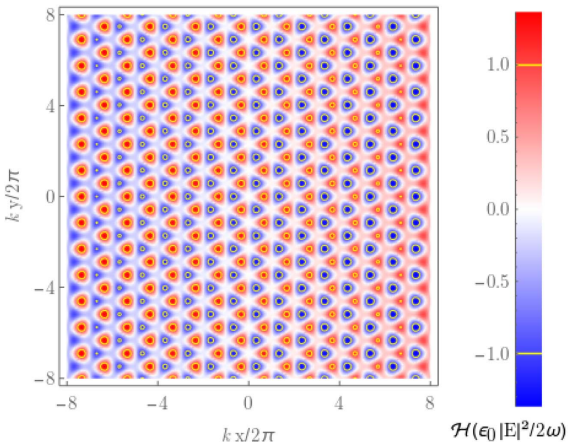

Fig. 7. Six-wave superposition for $\theta = \frac{2\pi}{3} - 0.005$ and $a_1 = a_2 = a_3$. For this angle, the helicity pattern is aperiodic in the x direction. The size of this plot is 16×16 wavelengths.

number of angles that satisfy this condition, yielding an infinite number of different lattices, with unit cells being allowed to become arbitrarily large. In Fig. 8 we give some examples of more complex helicity lattices.

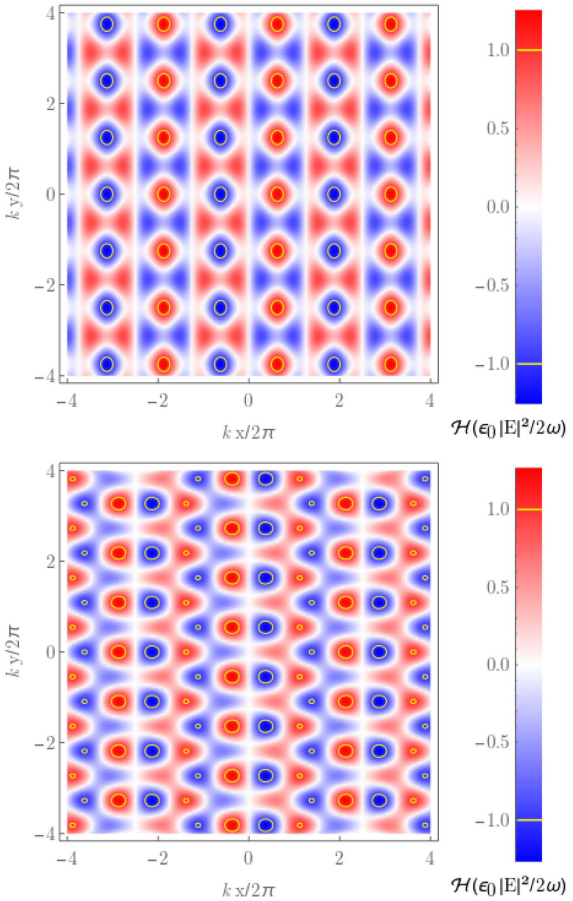

Fig. 8. Six-wave helicity lattice with $\theta = \arccos -\frac{3}{5}$ and $a_1 = a_2 = a_3$ (top) and with $\theta = \arccos -\frac{2}{5}$ and $a_1 = a_2 = a_3$ (bottom). The size of these plots is 8×8 wavelengths.

4. EFFECTS OF SMALL DEVIATIONS FROM THE EXACT PARAMETERS

Although the superpositions from the previous section have some parametric freedom left, the homogeneity of $\tilde{\mathbf{E}}^* \cdot \tilde{\mathbf{E}}$ depends on the fine-tuning of at least some parameters. These parameters can be any of the parameters that specify a plane wave: amplitude, phase, polarization, or/and propagation direction. The effects of misalignment in the propagation direction of the waves can be mitigated if the helicity lattice is of sufficiently small size and will be treated separately. Amplitude, phase, and polarization errors affect small lattices as well as big ones and can be treated in a unified picture.

A. Deviations in Amplitude, Phase, and Polarization

Deviations in the amplitudes, phases, and polarizations of the waves constituting a noninterfering superposition from their optimal values can be treated by writing the total electric field in the following way:

$$\tilde{\mathbf{E}} = \sum_{j=1}^{n} (\tilde{\mathbf{E}}_j + \delta\tilde{\mathbf{E}}_j) e^{i\mathbf{k}_j \cdot \mathbf{x}} \quad \text{with} \quad \delta\tilde{\mathbf{E}}_j \cdot \mathbf{k}_j = 0. \tag{5}$$

The different components of $\delta\tilde{\mathbf{E}}_j$ represent the different parameters. The component parallel to and with the same complex phase as $\tilde{\mathbf{E}}_j$ causes a deviation in the amplitude, the component parallel and $\frac{\pi}{2}$ out of phase represents phase deviations, the component perpendicular to and with the same complex phase as $\tilde{\mathbf{E}}_j$ represents errors in the polarization direction, and the perpendicular component $\frac{\pi}{2}$ out of phase represents deviations in the ellipticity. Each of these components can cause residual interference in $\tilde{\mathbf{E}}^* \cdot \tilde{\mathbf{E}}$ at first order in $\delta\tilde{\mathbf{E}}$. In general, the residual interference has the form

$$\delta I_{\mathbf{k}\neq 0} = \frac{1}{4} \sum_{j\neq l}^{n} (\delta\tilde{\mathbf{E}}_j^* \cdot \tilde{\mathbf{E}}_l + \tilde{\mathbf{E}}_j^* \cdot \delta\tilde{\mathbf{E}}_l) e^{i(\mathbf{k}_l - \mathbf{k}_j)\cdot \mathbf{x}} + O(\delta\tilde{\mathbf{E}}^2). \tag{6}$$

As a measure of the quality of the superpositions, we take the combined magnitude of all residual interference terms normalized by the homogeneous background field strength:

$$\frac{\sum_{j\neq l}^{n} \delta\tilde{\mathbf{E}}_j^* \cdot \tilde{\mathbf{E}}_l + \tilde{\mathbf{E}}_j^* \cdot \delta\tilde{\mathbf{E}}_l}{\sum_{l=1}^{n} \tilde{\mathbf{E}}_l^* \cdot \tilde{\mathbf{E}}_l} = \frac{(n-1)\langle |\delta\tilde{\mathbf{E}}_j^* \cdot \tilde{\mathbf{E}}_l| \rangle_{jl}}{\langle \tilde{\mathbf{E}}_l^* \cdot \tilde{\mathbf{E}}_l \rangle_l}. \tag{7}$$

Here, $\langle\rangle_l$ denotes averaging over all waves and $\langle\rangle_{jl}$ denotes averaging over all pairs of different waves. We make the additional assumption that the expectation value of $|\delta\tilde{\mathbf{E}}_j|$ is independent of its orientation. That is, all parameters have equally big errors. If this is not the case, one can set the errors in all parameters equal to the least well controlled one as a worst-case estimate. Then, as a worst-case estimate we have $\langle |\delta\tilde{\mathbf{E}}_j^* \cdot \tilde{\mathbf{E}}_l| \rangle_{jl} \leq \langle |\delta\tilde{\mathbf{E}}_j| \rangle_j \langle |\tilde{\mathbf{E}}_l| \rangle_l \times \frac{1}{2\pi} \int_0^{2\pi} \cos\theta \mathrm{d}\theta = \langle |\delta\tilde{\mathbf{E}}_j| \rangle_j \langle |\tilde{\mathbf{E}}_l| \rangle_l \frac{2}{\pi}$, giving an estimate for the residual interference of

$$\frac{2(n-1)\langle |\delta\tilde{\mathbf{E}}_j| \rangle_j \langle |\tilde{\mathbf{E}}_l| \rangle_l}{\pi \langle \tilde{\mathbf{E}}_l^* \cdot \tilde{\mathbf{E}}_l \rangle_l}. \tag{8}$$

From this equation one can see that the residual inhomogeneity of the helicity density is linear in polarization, phase, and polarization errors, and that superpositions of many waves are expected to have relatively larger helicity density inhomogeneities.

B. Deviations in the Propagation Direction

Deviations in the propagation direction can be described by replacing $\mathbf{k}_j$ with $\mathbf{k}_j + \delta\mathbf{k}_j$, where $\mathbf{k}_j \cdot \delta\mathbf{k}_j = 0$ to keep the frequency fixed. The effects of such deviations are twofold. First, if $\delta\mathbf{k}_j$ has a component parallel to $\tilde{\mathbf{E}}$, the light's polarization must rotate accordingly to preserve transversality, introducing a change in the electric field of $\delta\tilde{\mathbf{E}}_j = \tilde{\mathbf{E}}_j \cdot \delta\mathbf{k}_j / |\mathbf{k}_j|$. Second, a pair of supposedly cancelling interference terms does not cancel exactly anymore, leading to a beating pattern in the field strength. Around the nodes, the mean square of the electric field is relatively homogeneous, and one can have a finite size low-interference region of size L if

$$\delta\mathbf{k}_j < \frac{A_{\max}}{L A_{\text{int}}}, \tag{9}$$

with $A_{\max}$ the maximal tolerable amplitude of $\tilde{\mathbf{E}}^* \cdot \tilde{\mathbf{E}}$-fluctuations and A_{int} the amplitude of a single interference term.

5. RECORDING HELICITY PATTERNS WITH LIQUID CRYSTALS

Over the past 20 years a rich variety of liquid crystal polymers were discovered that become chiral under illumination with circularly polarized light [26–34]. The literature on the topic is far too broad to be covered here in full, but it suffices to note that the compounds that show this behavior are either polymers with long light-absorbing side chains that twist themselves into helices under illumination [26–28,30,32] or propeller-shaped molecules that can stack themselves in either a left- or a right-handed helix [31,33,34]. The permanence of the induced chirality varies a lot among compounds. Some have their chirality erased by illumination with the opposite polarization [28,30] or by heating [31], others can have their chirality fixated [34]. Light intensities used to achieve this chirality are on the order of tens or hundreds of milliwatts per square centimeter, and illumination takes up to an hour [28,30,34]. Several applications for these compounds have been tested, such as an optical polarization switch [35] and chiral second harmonic generation [33]. So far, these compounds were used in combination only with homogeneously polarized light. Helicity lattices can imprint an inhomogeneous chirality into a polymer film, making it possible to either use the polymer as "chiral" film to record the helicity structure of the light or to use the light to write helicity-sensitive optical components into a polymer film. For example, the helicity patterns from Fig. 8 can serve as arrays of chiral waveguides that guide light of one helicity only. The kind of polymer one would want for imprinting chiral structures is one that can chirally assemble under exposure with a helicity lattice and then have its supramolecular structure fixated by a process that works equally well on both enantiomers, yielding an imprint that remains stable at high temperatures and light intensities.

6. SOME REMARKS ON THE MATHEMATICS OF NONINTERFERING SUPERPOSITIONS

We have constructed superpositions with a homogeneous mean squared electric field of up to six plane waves. We do not know if there is an upper bound to the number of plane waves that can be superposed in this way, but we suspect there is, because the number of interference terms increases faster than the number of free parameters available.

We also noticed that whenever we superpose four or more plane waves either $\tilde{\mathbf{E}}^* \cdot \tilde{\mathbf{E}}$ or $\tilde{\mathbf{H}}^* \cdot \tilde{\mathbf{H}}$ is inhomogeneous. We believe there

cannot exist a superposition of four or more plane waves with both of them homogeneous, but we did not find a rigorous proof of this conjecture. We have similarly been unable to prove that when superposing three or more waves either $\tilde{\mathbf{E}}^* \cdot \tilde{\mathbf{E}}$, $\tilde{\mathbf{H}}^* \cdot \tilde{\mathbf{H}}$ or $\tilde{\mathbf{E}}^* \cdot \tilde{\mathbf{H}}$ is inhomogeneous, although we suspect this to be the case as well.

Every noninterfering superposition of four or more waves we know about has all light waves linearly polarized, and introducing elliptically polarized waves in any of them will lead to interference. This made us believe that all waves being linearly polarized is a requirement for every noninterfering superposition of four or more waves.

As far as we know, none of the above problems has been formulated before.

7. OUTLOOK

Apart from being an optics curiosity, noninterfering superpositions of more than three waves raise new mathematical challenges and provide new ways to probe and manipulate chiral matter. There is a large variety of possible helicity patterns, of which we have shown only a sample. For all helicity lattices, the lattice spacing scales with the wavelength of the light and there is no size limit other than the technical ability to superpose multiple coherent beams of light at the desired wavelength. One can imagine x-ray helicity lattices with unit cells the size of atoms or radio wave lattices with unit cells bigger than a house.

We are surprised at how common "bright region" superchirality is among noninterfering superpositions. We expect that it can occur as well if $\tilde{\mathbf{E}}^* \cdot \tilde{\mathbf{E}}$ is inhomogeneous, making a systematic study of this effect go well beyond the scope of this paper.

Funding. Engineering and Physical Sciences Research Council (EPSRC) (EP/M004694/1); Leverhulme Trust (RPG-2017-048); National Key Research and Development Program of China (2017YFA0303700).

Acknowledgment. RPC's contribution was supported by the EPSRC and the Leverhulme Trust. JBG's contribution was supported by the National Key Research and Development Program of China. We thank Ulf Saalmann for noticing the issue of robustness under small deviations from the optimal parameters.

REFERENCES

1. J. L. Trueba and A. F. Rañada, "The electromagnetic helicity," Eur. J. Phys. **17**, 141–144 (1996).
2. G. N. Afanasiev and Y. P. Stepanovski, "The helicity of the free electromagnetic field and its physical meaning," Nuovo Cim. A **109**, 271–279 (1996).
3. R. P. Cameron, S. M. Barnett, and A. M. Yao, "Optical helicity, optical spin and related quantities in electromagnetic theory," New J. Phys. **14**, 053050 (2012).
4. R. P. Cameron and S. M. Barnett, "Electric-magnetic symmetry and Noether's theorem," New J. Phys. **14**, 123019 (2012).
5. R. P. Cameron, S. M. Barnett, and A. M. Yao, "Optical helicity of interfering waves," J. Mod. Opt. **61**, 25–31 (2013).
6. Y. Tang and A. E. Cohen, "Optical chirality and its interaction with matter," Phys. Rev. Lett. **104**, 163901 (2010).
7. E. Hendry, T. Carpy, J. Johnston, M. Popland, R. V. Michailovski, A. J. Lapthorn, S. M. Kelly, L. D. Barron, N. Gadegaard, and M. Kadowala, "Ultrasensitive detection and characterization of biomolecules using superchiral fields," Nat. Nanotechnol. **5**, 783–787 (2010).
8. Y. Tang and A. E. Cohen, "Enhanced enantioselectivity in excitation of chiral molecules by superchiral light," Science **332**, 333–336 (2011).
9. C. Rosales-Guzmán, K. Volke-Sepulveda, and J. P. Torres, "Light with enhanced optical chirality," Opt. Lett. **37**, 3486–3488 (2012).
10. M. Schäferling, X. Yin, and H. Giessen, "Formation of chiral fields in a symmetric environment," Opt. Express **20**, 26326–26336 (2012).
11. M. Schäferling, X. Yin, N. Engheta, and H. Giessen, "Helical plasmonic nanostructures as prototypical chiral near-field sources," ACS Photon. **1**, 530–537 (2014).
12. X. Tian, Y. Fang, and M. Sun, "Formation of enhanced uniform chiral fields in symmetric dimer nanostructures," Sci. Rep. **5**, 17534 (2015).
13. M. Schäferling, N. Engheta, H. Giessen, and T. Weiss, "Reducing the complexity: enantioselective chiral near-fields by diagonal slit and mirror configuration," ACS Photon. **3**, 1076–1084 (2016).
14. C. Kramer, M. Schäferling, T. Weiss, H. Giessen, and T. Brixner, "Analytic optimization of near-field optical chirality enhancement," ACS Photon. **4**, 396–406 (2017).
15. L. Woltjer, "A theorem on force-free magnetic fields," Proc. Natl. Acad. Sci. USA **44**, 289–291 (1958).
16. M. G. Calkin, "An invariance property of the electric field," Am. J. Phys. **33**, 958–960 (1965).
17. K. C. van Kruining and J. B. Götte, "The conditions for the preservation of duality symmetry in a linear medium," J. Opt. **18**, 085601 (2016).
18. R. P. Cameron, S. M. Barnett, and A. M. Yao, "Discriminatory optical force for chiral molecules," New J. Phys. **16**, 013020 (2014).
19. A. Canaguier-Durand, J. A. Hutchison, C. Genet, and T. W. Ebbesen, "Mechanical separation of chiral dipoles by chiral light," New J. Phys. **15**, 123037 (2013).
20. S. K. Mohanty, K. D. Rao, and P. K. Gupta, "Optical trap with spatially varying polarization: application in controlled orientation of birefringent microscopic particle(s)," Appl. Phys. B **80**, 631–634 (2005).
21. G. Cipparrone, I. Ricardez-Vargas, P. Pagliusi, and C. Provenzano, "Polarization gradient: exploring an original route for optical trapping and manipulation," Opt. Express **18**, 6008–6013 (2010).
22. R. P. Cameron, A. M. Yao, and S. M. Barnett, "Diffraction gratings for chiral molecules and their applications," J. Phys. Chem. A **118**, 3472–3478 (2014).
23. K. Hornberger, S. Gerlich, H. Ulbricht, L. Hackermüller, S. Nimmrichter, I. V. Goldt, O. Botalina, and M. Arndt, "Theory and experimental verification of Kapitza-Dirac-Talbot-Lau interferometry," New J. Phys. **11**, 043032 (2009).
24. S. Eibenberger, S. Gerlich, M. Arndt, M. Mayor, and J. Tüxen, "Matter-wave interference of particles selected from a molecular library with masses exceeding 10,000 amu," Phys. Chem. Chem. Phys. **15**, 14696–14700 (2013).
25. R. P. Cameron, J. B. Götte, S. M. Barnett, and J. P. Cotter, "Matter-wave grating distinguishing conservative and dissipative interactions," Phys. Rev. A **94**, 013604 (2016).
26. L. Nikolova, T. Todorov, M. Ivanov, F. Andruzzi, S. Hvilsted, and P. Ramanujam, "Photoinduced circular anisotropy in side-chain azobenzene polyesters," Opt. Mater. **8**, 255–258 (1997).
27. L. Nikolova, L. Nedelchev, T. Todorov, T. Petrova, N. Tomova, V. Dragostinova, P. S. Ramanujam, and S. Hvilsted, "Self-induced light polarization rotation in azobenzene-containing polymers," Appl. Phys. Lett. **77**, 657–659 (2000).
28. G. Iftime, F. L. Labarthet, A. Natansohn, and P. Rochon, "Control of chirality of an azobenzene liquid crystalline polymer with circularly polarized light," J. Am. Chem. Soc. **122**, 12646–12650 (2000).
29. S.-W. Choi, T. Izumi, Y. Hoshino, Y. Takanishi, K. Ishikawa, J. Watanabe, and H. Takezoe, "Circular-polarization-induced enantiomeric excess in liquid crystals of an achiral, bent-shaped mesogen," Angew. Chem. **45**, 1382–1385 (2006).
30. R. M. Tejedor, L. Oriol, J. L. Serrano, F. Partal Ureña, and J. J. López González, "Photoinduced chiral nematic organization in an achiral glassy nematic azopolymer," Adv. Funct. Mater. **17**, 3486–3492 (2007).
31. F. Vera, R. M. Tejedor, P. Romero, J. Barberá, M. B. Ros, J. L. Serrano, and T. Sierra, "Light-driven supramolecular chirality in propeller-like hydrogen-bonded complexes that show columnar mesomorphism," Angew. Chem. **46**, 1873–1877 (2007).
32. J. D. Barrio, R. M. Tejedor, and L. Oriol, "Thermal and light control of the chiral order of azopolymers," Eur. Polym. J. **48**, 384–390 (2012).
33. L. de Vega, S. van Cleuvenbergen, G. Depotter, E. M. García-Frutos, B. Gómez-Lor, A. Omenat, R. M. Tejedor, J. L. Serrano, G. Hennrich, and K. Clays, "Nonlinear optical thin film device from a chiral octopolar phenylacetylene liquid crystal," J. Org. Chem. **77**, 10891–10896 (2012).
34. J. Kim, J. Lee, W. Y. Kim, H. Kim, S. Lee, H. C. Lee, Y. S. Lee, M. Seo, and S. Y. Kim, "Induction and control of supramolecular chirality by light in self-assembled helical nanostructures," Nat. Commun. **6**, 6959 (2015).
35. G. Martínez-Ponce, C. Solano, R. J. Rodríguez González, L. Larios-López, D. Navarro-Rodríguez, and L. Nikolova, "All-optical switching using supramolecular chiral structures in azopolymers," J. Opt. A **10**, 115006 (2008).